Multi-Fidelity Space Mapping Modeling of Microwave Devices with Double Coarse Model Processing and Functional Approximation

Slawomir Koziel[1], and John W. Bandler[2]

[1] School of Science and Engineering, Reykjavik University, Kringlunni 1, IS-103 Reykjavik, Iceland
[2]Department of Electrical & Computer Engineering, McMaster University, Hamilton, ON, Canada L8S 4K1
and Bandler Corporation, Dundas, ON, Canada L9H 5E7
[1] koziel@ru.is, [2] bandler@mcmaster.ca

***Abstract*—Efficient space mapping (SM) modeling of microwave devices assuming a tight limit on the number of fine model evaluations is discussed. The proposed method exploits a two-stage modeling procedure. The standard space mapping surrogate enhanced by a functional approximation layer using coarse-mesh EM simulation data is created in the first stage. This surrogate model is then updated in the second stage through space-mapping-based matching to the fine-mesh EM simulation responses at a limited number of base locations (designs). It is demonstrated that the proposed approach improves modeling accuracy in comparison to the standard SM method with no extra fine model evaluations required to set up the model.**

***Index Terms*—Computer-aided design (CAD), EM modeling, space mapping, surrogate modeling, functional approximation.**

I. Introduction

Fast and accurate models of microwave structures and devices are crucial in microwave engineering to perform tasks such as design optimization and statistical analysis. Demand for efficient models is particularly growing nowadays as microwave engineering relies more and more on computer-aided design. On the other hand, in creating such models we encounter the serious problem of the accurate evaluation of microwave structures that normally require CPU-intensive full-wave EM simulations.

There is a large group of functional approximation techniques that can be used to create fast surrogate models, including radial basis functions [1], kriging [2], fuzzy systems [3], and neural networks [4], [5], the latter probably being the most popular and successful approach in this group. In order to achieve good modeling accuracy, all of these methods require, however, a large amount of data obtained through massive EM simulations. Moreover, the number of data pairs necessary to ensure sufficient accuracy grows exponentially with the number of the design variables.

Another important modeling technique is space mapping (SM) [6], [7]. Space mapping constructs a surrogate model of a high fidelity CPU-intensive "fine" model by an enhancement of a computationally cheap "coarse" model through some auxiliary (usually linear) mappings. The parameters of these mappings are adjusted so that the surrogate matches the fine model as well as possible at limited numbers of base points (designs). Because the coarse model is supposedly physics-based, we hope that the matching will also be good over the whole region of interest.

It has been shown that the accuracy of the standard SM is almost independent of the amount of fine model data, i.e., increasing the number of base points over some limit (depending on SM mappings used in the surrogate model) has little or no influence on accuracy. Therefore, various combinations of SM with functional approximation techniques have been proposed [8]-[10] that retain the main advantages of space mapping and ensure increasing modeling accuracy if the amount of the available fine model data is also increasing. Although these approaches also suffer from the exponential dependence of the number of base points on the number design variables, the modeling accuracy of SM combined with functional approximation is better than the accuracy of purely functional models for an equivalent amount of training data.

Here, we consider a technique that allows improvement of modeling accuracy without increasing the number of base points, or equivalently, the number of high-fidelity EM simulations. Our technique is based on utilizing an "intermediate", coarse-mesh EM-based model. The data from this model is used to set up an initial surrogate exploiting both SM and functional approximation. This surrogate is subsequently enhanced by the standard SM approach with the model parameters being extracted through a small number of fine model base points. It is demonstrated that the resulting surrogate model exhibits better accuracy than the standard SM model, and the computational cost of creating both models is similar.

II. Standard Space Mapping Modeling

Let $\boldsymbol{R}_f : X_f \rightarrow R^m$, $X_f \subseteq R^n$, and $\boldsymbol{R}_c : X_c \rightarrow R^m$, $X_c \subseteq R^n$, denote the fine and coarse model response vectors. For example, $\boldsymbol{R}_f(\boldsymbol{x})$ and $\boldsymbol{R}_c(\boldsymbol{x})$ may represent the magnitude of a transfer function at m chosen frequencies. Let $X_R \subseteq X_f$ be a region of interest where we want enhanced matching between the surrogate and $\boldsymbol{R}_f$. Here, X_R is an n-dimensional interval in R^n with center at reference point $\boldsymbol{x}^0 = [x_{0.1} \ldots x_{0.n}]^T \in R^n$ and size $\boldsymbol{\delta} = [\delta_1 \ldots \delta_n]^T$ [7]. Let $X_B = \{\boldsymbol{x}^1, \boldsymbol{x}^2, \ldots, \boldsymbol{x}^N\} \subset X_R$ be the base set, such that the fine model response is known at all points $\boldsymbol{x}^j$, $j = 1, 2, \ldots, N$.

This work was supported in part by the Natural Sciences and Engineering Research Council of Canada under Grants RGPIN7239-06, STPGP336760-06, and by Bandler Corporation.

Let $\overline{\boldsymbol{R}}_s : X_R \times X_p \rightarrow R^m$ be a generic SM surrogate model where X_p is a parameter domain. For any given base set X_B the standard surrogate model $\boldsymbol{R}_{s.SM}$ is defined as

$$\boldsymbol{R}_{s.SM}(\boldsymbol{x}) = \overline{\boldsymbol{R}}_s(\boldsymbol{x}, \overline{\boldsymbol{p}}) \tag{1}$$

where

$$\overline{\boldsymbol{p}} = \arg\min_{\boldsymbol{p} \in X_p} \sum_{k=1}^{N} \| \boldsymbol{R}_f(\boldsymbol{x}^k) - \overline{\boldsymbol{R}}_s(\boldsymbol{x}^k, \boldsymbol{p}) \| \tag{2}$$

A variety of SM surrogate models is available [6], [7]. The model often used in practice (e.g., [7]) takes the form of $\overline{\boldsymbol{R}}_s(\boldsymbol{x}, \boldsymbol{p}) = \overline{\boldsymbol{R}}_s(\boldsymbol{x}, \boldsymbol{A}, \boldsymbol{B}, \boldsymbol{c}) = \boldsymbol{A} \cdot \boldsymbol{R}_c(\boldsymbol{B} \cdot \boldsymbol{x} + \boldsymbol{c})$ and employs both input and output SM. Note that the parameter extraction process (2) is independent of the evaluation point $\boldsymbol{x}$ of the surrogate model. This is the primary reason for which the modeling accuracy of the model (1)-(2) is barely dependent on the number of the base points N.

III. Multi-Fidelity Space Mapping Modeling

In this paper we propose a multi-fidelity SM-based modeling technique that allows us to improve modeling accuracy without increasing the number of fine model evaluations.

Let $\boldsymbol{R}_{f\text{-}c}$ denote the response of the intermediate fidelity model, typically a model evaluated using the same EM solver as the fine model $\boldsymbol{R}_f$ but with a coarser mesh. We assume that $\boldsymbol{R}_{f\text{-}c}$ is more accurate than the coarse model $\boldsymbol{R}_c$ but not as computationally expensive as the fine model.

Our technique is based on (i) setting up an initial surrogate $\boldsymbol{R}_{s.init}$ that is a good representation of the intermediate model $\boldsymbol{R}_{f\text{-}c}$, and (ii) enhancing $\boldsymbol{R}_{s.init}$ using the standard SM modeling approach and a limited number of fine model responses.

A. Initial Surrogate Model

The initial surrogate model $\boldsymbol{R}_{s.init}$ is defined as

$$\boldsymbol{R}_{s.init}(\boldsymbol{x}) = \overline{\boldsymbol{R}}_{s.1}(\boldsymbol{x}, \overline{\boldsymbol{p}}_1) + \tilde{\boldsymbol{R}}(\boldsymbol{x}) \tag{3}$$

where

$$\overline{\boldsymbol{p}}_1 = \arg\min_{\boldsymbol{p}_1} \sum_{k=1}^{N_1} \| \boldsymbol{R}_{f-c}(\boldsymbol{x}_{b1}^k) - \overline{\boldsymbol{R}}_{s.1}(\boldsymbol{x}_{b1}^k, \boldsymbol{p}_1) \| \tag{4}$$

Here, $\overline{\boldsymbol{R}}_{s.1}$ is a generic SM surrogate model (cf. Section II), $X_{B1} = \{\boldsymbol{x}_{b1}^1, \boldsymbol{x}_{b1}^2, \ldots, \boldsymbol{x}_{b1}^{N_1}\} \subset X_R$ is the base set, and $\tilde{\boldsymbol{R}}$ is a functional model that approximates the differences between $\boldsymbol{R}_{f\text{-}c}$ and $\overline{\boldsymbol{R}}_{s.1}$ at all base points.

In this paper, $\tilde{\boldsymbol{R}}$ is implemented using radial basis function (RBF) interpolation [1], [10]. Let $\boldsymbol{R}_{f\text{-}c}(\boldsymbol{x}) = [R_{f\text{-}c.1}(\boldsymbol{x}) \ \ldots \ R_{f\text{-}c.m}(\boldsymbol{x})]^T$ and $\overline{\boldsymbol{R}}_{s.1}(\boldsymbol{x}) = [\overline{R}_{s.1.1}(\boldsymbol{x}) \ \ldots \ \overline{R}_{s.1.m}(\boldsymbol{x})]^T$. $\tilde{\boldsymbol{R}}$ is defined as

$$\tilde{\boldsymbol{R}}(\boldsymbol{x}) = \begin{bmatrix} \sum_{j=1}^{N} \lambda_{1.j} \phi(\| \boldsymbol{x} - \boldsymbol{x}_{b1}^j \| / \gamma) \\ \ldots \\ \sum_{j=1}^{N} \lambda_{m.j} \phi(\| \boldsymbol{x} - \boldsymbol{x}_{b1}^j \| / \gamma) \end{bmatrix} \tag{5}$$

where $\| \cdot \|$ denotes the Euclidean norm. The parameters $\lambda_{k.j}$ are calculated so that they satisfy

$$\Phi \boldsymbol{\lambda}_k = \boldsymbol{F}_k \qquad k = 1, 2, \ldots, m \tag{6}$$

where $\boldsymbol{\lambda}_k = [\lambda_{k.1} \ \ \lambda_{k.2} \ \ \ldots \ \ \lambda_{k.N}]^T$,

$$\boldsymbol{F}_k = \begin{bmatrix} R_{f-c.k}(\boldsymbol{x}_{b1}^1) - \overline{R}_{s.1.k}(\boldsymbol{x}_{b1}^1) \\ \vdots \\ R_{f-c.k}(\boldsymbol{x}_{b1}^{N_1}) - \overline{R}_{s.1.k}(\boldsymbol{x}_{b1}^{N_1}) \end{bmatrix} \tag{7}$$

and Φ is an $N \times N$ matrix with elements

$$\Phi_{ij} = \phi(\| \boldsymbol{x}^i - \boldsymbol{x}^j \| / \gamma) \tag{8}$$

$\gamma = [2/(nN_1^{1/n})] \sum_{i=1}^{n} \delta_i$ is a normalization factor (an average distance between the base points). Here, we use a Gaussian basis function defined as

$$\phi(r) = e^{-cr^2} \qquad r \geq 0 \qquad c > 0 \tag{9}$$

B. Space Mapping Enhancement of the Initial Surrogate

The final surrogate model $\boldsymbol{R}_s$ is defined as the standard SM-based enhancement of $\boldsymbol{R}_{s.init}$, i.e.,

$$\boldsymbol{R}_s(\boldsymbol{x}) = \overline{\boldsymbol{R}}_{s.2}(\boldsymbol{x}, \overline{\boldsymbol{p}}_2) \tag{10}$$

where

$$\overline{\boldsymbol{p}}_2 = \arg\min_{\boldsymbol{p}_2} \sum_{k=1}^{N_2} \| \boldsymbol{R}_f(\boldsymbol{x}_{b2}^k) - \overline{\boldsymbol{R}}_{s.2}(\boldsymbol{x}_{b2}^k, \boldsymbol{p}_2) \| \tag{11}$$

Here, $\overline{\boldsymbol{R}}_{s.2}$ is a generic SM surrogate model that can be the same or different than $\overline{\boldsymbol{R}}_{s.1}$ and $X_{B2} = \{\boldsymbol{x}_{b2}^1, \boldsymbol{x}_{b2}^2, \ldots, \boldsymbol{x}_{b2}^{N_2}\} \subset X_R$ is the base set.

C. Practical Issues

The functional approximation layer $\tilde{\boldsymbol{R}}$ is used in (3) to ensure that $\boldsymbol{R}_{s.init}$ is a good representation of $\boldsymbol{R}_{f\text{-}c}$. In particular, unlike the standard SM, RBF model (5)-(8) guarantees that the modeling error $\|\boldsymbol{R}_{s.init}(\boldsymbol{x}) - \boldsymbol{R}_{f\text{-}c}(\boldsymbol{x})\|$ is as small as required over X_R provided that the number of base points N_1 is sufficiently large. On the other hand, the accuracy of the combined SM-RBF model (3) is much better than the accuracy of the stand-alone RBF model [10].

The number of base points N_2 is normally much smaller than N_1 because the idea of multi-fidelity modeling is based on the assumption that $\boldsymbol{R}_{s.init}$ is already a much better representation of the fine model than the coarse model, and also because we want to keep the number of fine model evaluations necessary to set up the surrogate model small.

For the purpose of numerical comparison with the standard SM model $\boldsymbol{R}_{s.SM}$, we will use $N_2 = N$ so that the cost of setting up models $\boldsymbol{R}_{s.SM}$ and $\boldsymbol{R}_s$ is the same in terms of the number of fine model evaluations.

III. Verification Examples

A. Third-Order Chebyshev Bandpass Filter [11]

Consider a third-order Chebyshev bandpass filter [11] (Fig. 1). The design parameters are $\boldsymbol{x} = [L_1 \ L_2 \ S_1 \ S_2]^T$ mm. Other parameters are: $W_1 = W_2 = 0.4$ mm. The fine model $\boldsymbol{R}_f$ is simulated in Sonnet ***em*** [12] with a fine grid of 0.2 mm × 0.02 mm. The coarse model $\boldsymbol{R}_c$, Fig. 2, is implemented in Agilent ADS [13]. The coarse-mesh model $\boldsymbol{R}_{f\text{-}c}$ is simulated in Sonnet ***em*** using a coarse grid of 2 mm × 0.2 mm. Simulation times for models $\boldsymbol{R}_f$, $\boldsymbol{R}_{f\text{-}c}$ and $\boldsymbol{R}_c$ are 10 minutes, 14 seconds and a few milliseconds, respectively.

For this example, the region of interest is defined as $\boldsymbol{x}^0 = [14\ 14\ 0.6\ 0.6]^T$ mm $\boldsymbol{\delta} = [2\ 2\ 0.2\ 0.2]^T$ mm, which is quite a large deviation (±15% for lengths and ±33% for spacing).

The standard SM surrogate $\boldsymbol{R}_{s.SM}$ has been set up using $N = 9$ base points allocated according to the star distribution [7]. The model uses an SM surrogate of the form $\boldsymbol{A}\cdot\boldsymbol{R}_c(\boldsymbol{B}\cdot\boldsymbol{x}+\boldsymbol{c})$.

The multi-fidelity model $\boldsymbol{R}_s$ is set up as follows. The initial surrogate $\boldsymbol{R}_{s.init}$ uses an SM surrogate of the form $\bar{\boldsymbol{R}}_{s.1} = \boldsymbol{A}\cdot\boldsymbol{R}_c(\boldsymbol{B}\cdot\boldsymbol{x}+\boldsymbol{c})$. The base set X_{B1} has $N_1 = 3^4 = 81$ points allocated as a uniform grid of density 3 with points at the corners, edges and faces of the region of interest. Note that the total evaluation time of $\boldsymbol{R}_{f\text{-}c}$ corresponds to less than two evaluations of the fine model. The final surrogate model $\boldsymbol{R}_s$ is defined using the same SM type, i.e., $\bar{\boldsymbol{R}}_{s.2} = \boldsymbol{A}\cdot\boldsymbol{R}_c(\boldsymbol{B}\cdot\boldsymbol{x}+\boldsymbol{c})$. The base set X_{B2} is the same as X_B, in particular, $N_2 = N$, i.e., the number of fine model evaluations necessary to set up $\boldsymbol{R}_s$ is the same as for $\boldsymbol{R}_{s.SM}$.

The modeling accuracy has been verified using 50 test points allocated randomly in the region of interest. Table I shows the average and maximum modeling error. Here, we use the relative error measure $||\boldsymbol{R}_f(\boldsymbol{x}) - \boldsymbol{R}_{surr}(\boldsymbol{x})||/||\boldsymbol{R}_f(\boldsymbol{x})||$ expressed in percent, where $\boldsymbol{R}_f(\boldsymbol{x})$ and $\boldsymbol{R}_{surr}(\boldsymbol{x})$ denote the fine and the respective surrogate model response at a given test point $\boldsymbol{x}$ (i.e., $\boldsymbol{R}_{surr}(\boldsymbol{x})$ is either $\boldsymbol{R}_{s.SM}(\boldsymbol{x})$ or $\boldsymbol{R}_s(\boldsymbol{x})$).

As indicated in Table I, the modeling error of the new multi-fidelity surrogate is almost two times smaller than the error of the standard SM model and the number of fine model evaluations, 9, is the same for both models.

It should be emphasized that the error values in Table I are very low considering the small number of fine model evaluations. This error level cannot be achieved by any of the existing functional approximation techniques using such a small number of base points (here, 9).

Figure 3 shows the error plots $|\boldsymbol{R}_f(\boldsymbol{x}) - \boldsymbol{R}_{surr}(\boldsymbol{x})|$ versus frequency for the standard SM surrogate and the new multi-fidelity model. Figure 4 shows the fine model response and the surrogate model responses at one of the test points.

B. Double Folded Stub Filter [14]

Consider a double folded stub (DFS) bandstop filter [14] (Fig. 5). The design parameters are $\boldsymbol{x} = [L_1\ L_2\ S]^T$ mil; W is set to 5 mil. The fine model $\boldsymbol{R}_f$ is simulated in Sonnet ***em*** [12] with a fine grid of 1 mil × 0.2 mil. The coarse model $\boldsymbol{R}_c$, Fig. 6, is implemented in Agilent ADS [13]. The coarse-mesh model $\boldsymbol{R}_{f\text{-}c}$ is simulated in Sonnet ***em*** using a coarse grid of 5 mil × 1 mil. Simulation times for models $\boldsymbol{R}_f$, $\boldsymbol{R}_{f\text{-}c}$ and $\boldsymbol{R}_c$ are 11 minutes, 22 seconds and a few milliseconds, respectively.

For this example, the region of interest is defined as $\boldsymbol{x}^0 = [90\ 85\ 8]^T$ mil $\boldsymbol{\delta} = [10\ 10\ 2]^T$ mil, which is about ±12% deviation for lengths and ±25% deviation for spacing.

The standard SM surrogate model $\boldsymbol{R}_{s.SM}$ has been set up using $N = 7$ base points allocated according to the star distribution [7]. The model uses an SM surrogate of the form $\boldsymbol{A}\cdot\boldsymbol{R}_c(\boldsymbol{B}\cdot\boldsymbol{x}+\boldsymbol{c})$ enhanced by frequency space mapping [7].

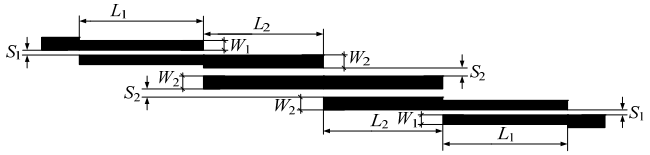

Fig. 1. Third-order Chebyshev bandpass filter [11].

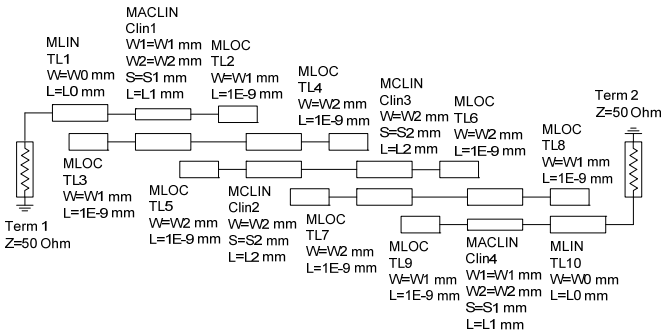

Fig. 2. Coarse model $\boldsymbol{R}_c$ of the third-order Chebyshev filter (Agilent ADS).

TABLE I
MODELING RESULTS FOR THIRD-ORDER CHEBYSHEV FILTER

Model	Average Error	Maximum Error
$\boldsymbol{R}_{s.SM}$	6.5 %	11.1 %
$\boldsymbol{R}_s$	3.8 %	7.0 %

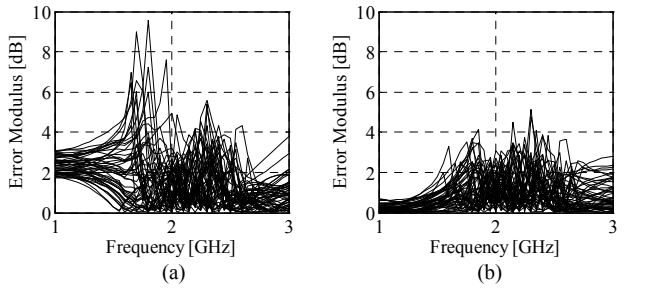

Fig. 3. Error plots for the third-order Chebyshev filter: (a) standard SM surrogate model $\boldsymbol{R}_{s.SM}$, and (b) multi-fidelity surrogate $\boldsymbol{R}_s$.

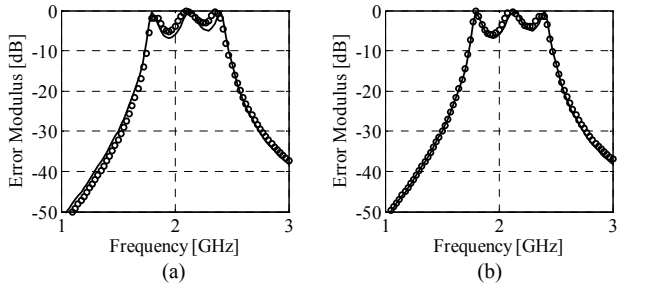

Fig. 4. Fine model (solid line) and the surrogate model (circles) response for at a selected test point for (a) standard SM surrogate model $\boldsymbol{R}_{s.SM}$, and (b) multi-fidelity surrogate $\boldsymbol{R}_s$.

The initial surrogate $\boldsymbol{R}_{s.init}$ uses a surrogate of the form $\bar{\boldsymbol{R}}_{s.1} = \boldsymbol{A}\cdot\boldsymbol{R}_c(\boldsymbol{B}\cdot\boldsymbol{x}+\boldsymbol{c})$ enhanced by frequency SM, and the base set X_{B1} has $N_1 = 5^3 = 125$ points allocated as a uniform grid of density 5. The total evaluation time of $\boldsymbol{R}_{f\text{-}c}$ corresponds to about four evaluations of $\boldsymbol{R}_f$. The final surrogate model $\boldsymbol{R}_s$ is defined using $\bar{\boldsymbol{R}}_{s.2} = \bar{\boldsymbol{R}}_{s.1}$ and $X_{B2} = X_B$.

Modeling accuracy has been verified using 50 test points allocated randomly in the region of interest and the same relative error measure as defined in Section III.*A*. Table II shows the average and maximum modeling error. The modeling accuracy is 2.5 times better for the new multi-fidelity surrogate than for the standard SM model.

Figure 7 shows the error plots $|\boldsymbol{R}_f(\boldsymbol{x}) - \boldsymbol{R}_{surr}(\boldsymbol{x})|$ versus frequency for the standard SM surrogate and the new multi-fidelity model.

As an application example, the surrogate model was used to optimize the DFS filter with respect to the design specifications $|S_{21}| \geq -20$ dB for 11.5 GHz $\leq \omega \leq$ 14.5 GHz, and $|S_{21}| \leq -3$ dB for 6.0 GHz $\leq \omega \leq$ 9.5 GHz and 16.5 GHz $\leq \omega \leq$ 20.0 GHz. Figure 8 shows the fine model responses at the starting point, $\boldsymbol{x}^0 = [90\ \ 85\ \ 8]^T$ mil (specification error +2.3 dB), and optimized design $\boldsymbol{x}_s$ of $\boldsymbol{R}_s$, $\boldsymbol{x}_s = [89\ \ 85\ \ 6]^T$ mil (specification error –0.2 dB).

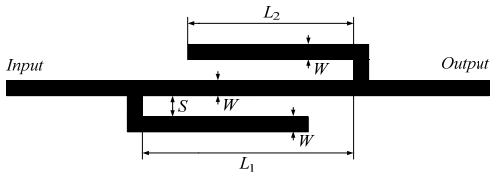

Fig. 5. Double folded stub bandstop filter [14].

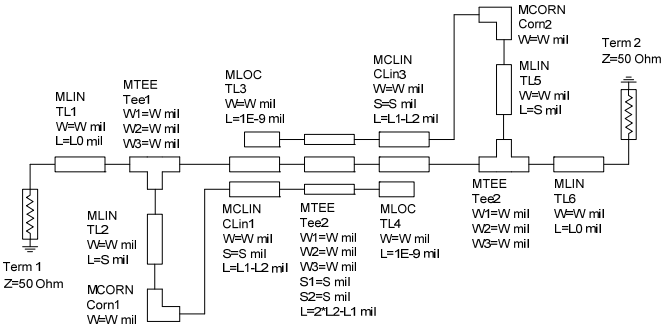

Fig. 6. Coarse model $\boldsymbol{R}_c$ of the double folded stub filter (Agilent ADS).

TABLE II
MODELING RESULTS FOR DOUBLE FOLDED STUB FILTER

Model	Average Error	Maximum Error
$\boldsymbol{R}_{s.SM}$	2.0 %	3.8 %
$\boldsymbol{R}_s$	0.8 %	1.9 %

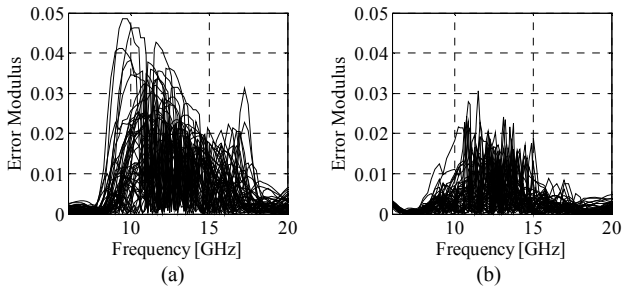

Fig. 7. Error plots for the double folded stub bandstop filter: (a) standard SM surrogate model $\boldsymbol{R}_{s.SM}$, and (b) multi-fidelity surrogate $\boldsymbol{R}_s$.

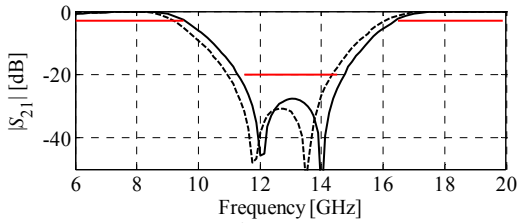

Fig. 8. Fine model response at $\boldsymbol{x}^0 = [90\ \ 85\ \ 8]^T$ mil (dashed line) and at the optimal design $\boldsymbol{x}_s = [89\ \ 85\ \ 6]^T$ mil of the surrogate model $\boldsymbol{R}_s$ (solid line).

IV. CONCLUSION

A new multi-fidelity modeling methodology is presented that combines SM with a functional approximation of the coarse-mesh EM-based model. This combination allows us to reduce the modeling error without increasing the number of fine model evaluations necessary to set up the surrogate model.

REFERENCES

[1] M.D. Buhmann and M. J. Ablowitz, *Radial Basis Functions: Theory and Implementations*, Cambridge University, 2003.

[2] W.C.M. van Beers and J.P.C. Kleijnen, "Kriging interpolation in simulation: survey," *Proc. 2004 Winter Simulation Conf.*, pp. 113-121, Washington, DC, USA, 2004.

[3] V. Miraftab and R.R. Mansour, "A robust fuzzy-logic technique for computer-aided diagnosis of microwave filters," *IEEE Trans. Microwave Theory Tech.*, vol. 52, no. 1, pp. 450-456, Jan. 2004.

[4] J.E. Rayas-Sánchez and V. Gutiérrez-Ayala, "EM-based Monte Carlo analysis and yield prediction of microwave circuits using linear-input neural-output space mapping," *IEEE Trans. Microwave Theory Tech.*, vol. 54, no. 12, pp. 4528-4537, Dec. 2006.

[5] X. Ding, V.K. Devabhaktuni, B. Chattaraj, M.C.E. Yagoub, M. Doe, J.J. Xu, and Q.J. Zhang, "Neural network approaches to electromagnetic based modeling of passive components and their applications to high-frequency and high-speed nonlinear circuit optimization," *IEEE Trans. Microwave Theory Tech.*, vol. 52, no. 1, pp. 436-449, Jan. 2004.

[6] J.W. Bandler, N. Georgieva, M.A. Ismail, J.E. Rayas-Sánchez, and Q. J. Zhang, "A generalized space mapping tableau approach to device modeling," *IEEE Trans. Microwave Theory Tech.*, vol. 49, no. 1, pp. 67-79, Jan. 2001.

[7] S. Koziel, J.W. Bandler, A.S. Mohamed, and K. Madsen, "Enhanced surrogate models for statistical design exploiting space mapping technology," *IEEE MTT-S Int. Microwave Symp. Dig.*, Long Beach, CA, June 2005, pp. 1609-1612.

[8] S. Koziel, J.W. Bandler, and K. Madsen, "Theoretical justification of space-mapping-based modeling utilizing a data base and on-demand parameter extraction," *IEEE Trans. Microwave Theory Tech.*, vol. 54, no. 12, pp. 4316-4322, Dec. 2006.

[9] S. Koziel and J.W. Bandler, "A space-mapping approach to microwave device modeling exploiting fuzzy systems," *IEEE Trans. Microwave Theory and Tech.*, vol. 55, no. 12, pp. 2539-2547, Dec. 2007.

[10] S. Koziel and J.W. Bandler, "Modeling of microwave devices with space mapping and radial basis functions," *Int. J. Numerical Modelling*, vol. 21, no. 3, pp. 187-203, 2008.

[11] J. T. Kuo, S. P. Chen, and M. Jiang, "Parallel-coupled microstrip filters with over-coupled end stages for suppression of spurious responses," *IEEE Microwave and Wireless Comp. Lett.*, vol. 13, no. 10, pp. 440-442, Oct. 2003.

[12] ***em***™ Version 11.53, Sonnet Software, Inc., 100 Elwood Davis Road, North Syracuse, NY 13212, USA, 2008.

[13] Agilent ADS, Version 2008, Agilent Technologies, 1400 Fountaingrove Parkway, Santa Rosa, CA 95403-1799, 2008.

[14] J.W. Bandler, R.M. Biernacki, S.H. Chen, P.A. Grobelny, and R.H. Hemmers, "Space mapping technique for electromagnetic optimization," *IEEE Trans. Microwave Theory Tech.*, vol. 4, no. 12, pp. 536-544, Dec. 1994.